A Robust Adaptive Dynamic Surface Control for Nonlinear Systems with Hysteresis Input

ZHANG Xiu-Yu[1] LIN Yan[1]

Abstract In this paper, a robust adaptive dynamic surface control (DSC) for a class of uncertain perturbed strict-feedback nonlinear systems preceded by unknown backlash-like hysteresis is proposed. The main advantages of our scheme are that it can eliminate the explosion of complexity problem when the hysteresis is fused with backstepping design, and by introducing an initializing technique, and the $\mathcal{L}_\infty$ performance of system tracking error can be guaranteed. It is proved that the new scheme can guarantee semiglobal stability of the closed-loop system and make the convergence of the tracking error into an arbitrarily small residual set. Simulation results are presented to demonstrate the efficiency of the proposed scheme.

Key words Dynamic surface control (DSC), backlash-like hysteresis, adaptive control, backstepping

DOI 10.3724/SP.J.1004.2010.01264

As one of the most important non-smooth nonlinearities, hysteresis exists in many physical systems and devices[1−4]. It is well known that when a plant is preceded by hysteresis nonlinearity, the system may exhibit undesirable properties such as inaccuracy, oscillations, and instability[5]. Indeed, modeling and control of hysteresis have long been challenging issues and have attracted a lot of attention in recent years due to increasing applications of smart material-based actuators[6−9].

The research dealing with hysteresis in control systems can be classified into two categories: one is to construct an inverse operator to cancel the hysteresis effect, and the other one is to develop some robust adaptive schemes without constructing hysteresis inverse. The first category, which as some authors pointed out[10], always possesses strong sensitivity of the model parameters to unknown measurement errors and, therefore, is directly linked to the difficulty of system stability analysis except for certain special cases, e.g. the method by Tao and Kokotovic[5] (for more details, see [5, 8−9, 11−12] and the references contained therein). While the second one has drawn much interest from the control community in recent years since it allows the designer to use various robust control schemes to mitigate the effect of hysteresis and makes the stability analysis more convenient[13−15]. In [14] and [16], for a class of nonlinear plants preceded by hysteresis, based on backlash-like hysteresis model, a robust adaptive control scheme was proposed, which achieves stabilization and tracking to certain precision without constructing a hysteresis inverse. In [16], some assumptions upon the controlled plant in [14] were relaxed by using backstepping design. In [13], combining variable structure and backstepping techniques, a robust adaptive control was applied to the case of hysteresis described by P-I model without constructing a hysteresis inverse. In [17], the adaptive control problem of a linear discrete time plant preceded by hysteresis was discussed. In [18], by using generalized P-I hysteresis model, for a class of uncertain nonlinear systems in pure-feedback form, an adaptive backstepping neural control scheme was introduced, where the uncertainties are compensated by using neural networks and the unknown virtual control directions are dealt with by using Nassbaum functions.

Manuscript received July 16, 2009; accepted December 29, 2009
Supported by National Natural Science Foundation of China (60874044) and Research Foundation for Key Disciplines of Beijing Municipal Commission of Education (XK100060422)
1. School of Automation, Beijing University of Aeronautics and Astronautics, Beijing 100191, P. R. China

We note that most of the above schemes without constructing hysteresis inverse are fused with adaptive backstepping control, which has been investigated extensively for the past two decades and become a popular design technique for a large class of nonlinear systems[19]. However, the main drawback of the backstepping design is that it suffers from the problem of "explosion of complexity". In other words, the control law becomes highly nonlinear and complicated as plant relative degree is high due to the repeated derivatives of certain modelled nonlinear functions. Obviously, the complexity problem may become more severe if a controlled plant with higher relative degree is preceded by hysteresis.

To overcome the drawback of backstepping design, inspired by the multiple surface sliding control, a new technique named dynamic surface control (DSC) was proposed by Swaroop et al. recently[20], which introduces a low-pass filter at each design step to prevent the derivative of nonlinear functions and, therefore, eliminates the phenomenon of explosion of complexity. The DSC technique has also been applied to some commonly encountered nonlinearities. In [21], for a class of pure-feedback nonlinear systems with unknown dead zone and perturbed uncertainties, an adaptive DSC was developed by using neural networks, whereas in [22], DSC technique was extended to state time delay uncertain nonlinear systems in parametric strict-feedback form. The latest developments in DSC for different nonlinear systems and the applications to various engineering fields can be referred to [23−26]. However, no systematic procedure exists for current DSC schemes to guarantee the transient performance of the tracking error.

In this paper, an adaptive DSC scheme is proposed for a class of nonlinear systems preceded by backlash-like hysteresis with the following features:

1) Within our knowledge, this is the first attempt to fuse backlash-like hysteresis with adaptive DSC for perturbed strict feedback nonlinear systems without constructing hysteresis inverse. Besides, it can also be extended to P-I and generalized P-I hysteresis models.

2) Compared with the backstepping control schemes concerning hysteresis[13, 16, 18], the explosion of complexity problem is eliminated.

3) By introducing an initializing technique, the $\mathcal{L}_\infty$ performance of system-tracking error can be guaranteed, which establishes the relationship between the $\mathcal{L}_\infty$ performance and the design parameters for the first time.

We point out that the elimination of the explosion of complexity is achieved by introducing a low-pass filter at each design step so that the differentiation of some nonlinear functions can be avoided. In addition, the class of perturbed strict-feedback nonlinear systems considered in this paper is of more general form and, therefore, is more suitable for applications.

1 Problem statement

We consider the following nonlinear plants in perturbed strict-feedback form preceded by backlash-like hysteresis actuator:

$$\begin{aligned}\dot{x}_i &= g_i x_{i+1} + \theta_i f_i(\bar{x}_i) + \Delta_i(x,t), \quad i = 1,\cdots,n-1\\ \dot{x}_n &= g_n w(t) + \theta_n f_n(x) + \Delta_n(x,t) + \bar{d}(t)\\ y &= x_1\end{aligned} \tag{1}$$

where $\bar{x}_i = [x_1, x_2, \cdots, x_i]^{\rm T} \in \mathbf{R}^i$, $i = 1, \cdots, n$ are the state vectors with $\bar{x}_n = x$; g_i, $\theta_i \in \mathbf{R}$ are unknown constant system parameters; Δ_i denotes the unknown perturbed terms; $y \in \mathbf{R}$ is the output of the controlled plant; $\bar{d}$ denotes an external disturbance; $w \in \mathbf{R}$ is the unknown backlash-like hysteresis and can be expressed as

$$w(t) = P(u(t)) \tag{2}$$

with u as the input signal to be designed.

For the controlled plant (1), we make the following assumptions.

Assumption 1. $f_i(\bar{x}_i)$, $i = 1, \cdots, n$ are known smooth functions.

Assumption 2. The disturbance terms $\Delta_i(x,t)$, $i = 1, \cdots, n$ satisfy

$$|\Delta_i(x,t)| \le \rho_i(\bar{x}_i) \tag{3}$$

where $\rho_i(\bar{x}_i)$ are known positive smooth functions.

Assumption 3. The desired trajectory y_r is smooth and available with $y_r(0)$ at designer's disposal; $[y_r, \dot{y}_r, \ddot{y}_r]^{\rm T}$ belongs to a known compact set for all $t \ge 0$.

Assumption 4. The signs of g_i, $i = 1, \cdots, n$ are known. Without loss of generality, it is assumed that $g_i > 0$. Moreover, it is assumed that $0 < g_{\min} \le |g_i| \le g_{\max}$ with $g_{\min}$ a known constant.

Assumption 5. The unmeasured disturbance $\bar{d}$ is bounded.

Remark 1. $y_r(0)$ in Assumption 3 will be employed to guarantee the $\mathcal{L}_\infty$ performance of system-tracking error. Assumption 4 is common for a large class of nonlinear systems[21−22].

In this paper, the backlash-like hysteresis nonlinearity is described by the following differential equation[14]:

$$\frac{{\rm d}w}{{\rm d}t} = \alpha \left|\frac{{\rm d}u}{{\rm d}t}\right| (\lambda u - w) + \psi \frac{{\rm d}u}{{\rm d}t} \tag{4}$$

where α, $\lambda\,(>0)$, and ψ are unknown constant parameters with $\lambda > \psi$. The solution of (4) is

$$w = \lambda u + d_1 \tag{5}$$

$$d_1(u) = (w_0 - \lambda u_0)\exp[-\alpha(u - u_0){\rm sgn}(\dot{u})] + \exp(-\alpha u\,{\rm sgn}(\dot{u})) \times \int_{u_0}^{u} (\psi - \lambda)\exp[\alpha\xi\,{\rm sgn}(\dot{u})]{\rm d}\xi \tag{6}$$

where $u_0 = u(t_0)$ and $w_0 = w(u_0)$. It can be proved that $d_1(u)$ is bounded for any $u \in \mathbf{R}$; furthermore,

$$\lim_{u\to-\infty} d_1(u) = \lim_{u\to-\infty}[w(u; u_0, w_0) - \lambda u] = \frac{\lambda - \psi}{\alpha} \tag{7}$$

$$\lim_{u\to+\infty} d_1(u) = \lim_{u\to+\infty}[w(u; u_0, w_0) - \lambda u] = -\frac{\lambda - \psi}{\alpha} \tag{8}$$

that is, α determines the rate at which w switches between $-(\lambda - \psi)/\alpha$ and $(\lambda - \psi)/\alpha$, i.e., the larger the parameter α is, the faster the transition frequency in w is going to be[14]. Fig. 1 illustrates the class of backlash-like hysteresis described by (4).

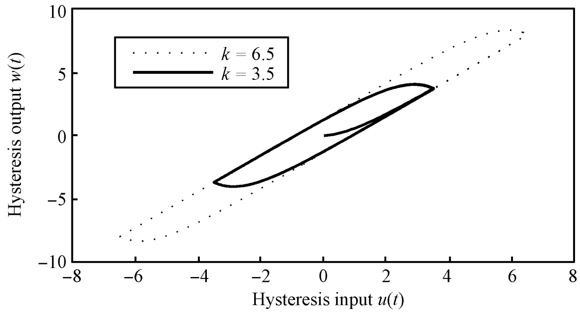

Fig. 1 Hysteresis curves given by (4), where the parameters $\alpha = 1$, $\lambda = 1.432$, $\psi = 0.105$, and the input $u(t) = k\sin(2.3t)$ with $k = 3.5$ and $k = 6.5$, respectively

Taking (5) into consideration, (1) can be rewritten as

$$\begin{aligned}\dot{x}_i &= g_i x_{i+1} + \theta_i f_i(\bar{x}_i) + \Delta_i(x,t), \quad i = 1,\cdots,n-1\\ \dot{x}_n &= \beta u + \theta_n f_n(\bar{x}_n) + \Delta_n(x,t) + d_n\\ y &= x_1\end{aligned} \tag{9}$$

where

$$\beta = \lambda g_n,\ \beta > 0 \tag{10}$$

$$d_n = g_n d_1(u) + \bar{d} \tag{11}$$

with d_n a bounded disturbance-like term satisfying

$$|d_n| \le d \tag{12}$$

where d is an unknown constant parameter. And as will be shown in the next section, both β and d will be online estimated.

The objective is to design the control law u in (9) based on DSC technique, such that the output y tracks a given reference input y_r with a prescribed small error and all the closed-loop signals are uniformly bounded.

Remark 2. We emphasize that system (1) can be used to describe many practical nonlinear systems preceded by unknown hysteresis such as pneumatic servomechanism[27], permanent magnet synchronous motor (PMSM)[25], and the systems with smart material-based actuators[2].

2 Adaptive DSC design

In this section, an adaptive DSC technique will be proposed to cope with the class of nonlinear systems with unknown backlash-like hysteresis described by (9). The whole design procedure contains n steps, and the actual control law u will be deduced in the last step.

Step 1. Let the first surface error be defined as

$$S_1 = x_1 - y_r \tag{13}$$

where y_r is the desired trajectory. Taking (9) into consideration, the derivative of S_1 is

$$\dot{S}_1 = \dot{x}_1 - \dot{y}_r = g_1 x_2 + \theta_1 f_1(x_1) + \Delta_1 - \dot{y}_r \tag{14}$$

Let

$$\theta_{g_1} = \frac{\theta_1}{g_1}$$
$$\phi_1 = \frac{1}{g_1} \tag{15}$$

Based on (14) and (15), a virtual control signal is chosen as

$$x_{2d} = -\hat{\theta}_{g_1} f_1(x_1) - \frac{1}{g_{\min}} \frac{S_1 \rho_1^2(x_1)}{2\varepsilon} - k_1 S_1 + \hat{\phi}_1 \dot{y}_r \tag{16}$$

where ε is any positive constant and, $\hat{\theta}_{g_1}$ and $\hat{\phi}_1$, which are the estimations of θ_{g_1} and ϕ_1, are updated by

$$\dot{\hat{\theta}}_{g_1} = \gamma_{g_1}(f_1(x_1)S_1 - \eta_1 \hat{\theta}_{g_1})$$
$$\dot{\hat{\phi}}_1 = -\gamma_{\phi_1}(\dot{y}_r S_1 + \sigma_1 \hat{\phi}_1) \tag{17}$$

with γ_{g_1}, η_1, γ_{ϕ_1}, σ_1 being positive design parameters. Let x_{2d} pass through a first-order filter to obtain z_2:

$$\tau_2 \dot{z}_2 + z_2 = x_{2d}, \quad z_2(0) = x_{2d}(0) \tag{18}$$

where τ_2 is the time constant.

Step i ($2 \le i \le n-1$). Define the i-th surface error

$$S_i = x_i - z_i - c_i \tag{19}$$

where c_i is a constant design parameter[1]. The time derivative of (19) is

$$\dot{S}_i = \dot{x}_i - \dot{z}_i = g_i x_{i+1} + \theta_i f_i(\bar{x}_i) + \Delta_i - \dot{z}_i \tag{20}$$

where the i-th equation in (9) has been used. Let

$$\theta_{g_i} = \frac{\theta_i}{g_i}$$
$$\phi_i = \frac{1}{g_i} \tag{21}$$

Based on (20) and (21), a virtual control signal is chosen as

$$x_{(i+1)d} = -\hat{\theta}_{g_i} f_i(\bar{x}_i) - \frac{1}{g_{\min}} \frac{S_i \rho_i^2(\bar{x}_i)}{2\varepsilon} - k_i S_i + \hat{\phi}_i \dot{z}_i \tag{22}$$

where $\hat{\theta}_{g_i}$ and $\hat{\phi}_i$, which are the estimations of θ_{g_i} and ϕ_i, respectively, are updated by

$$\dot{\hat{\theta}}_{g_i} = \gamma_{g_i}(f_i(\bar{x}_i)S_i - \eta_i \hat{\theta}_{g_i})$$
$$\dot{\hat{\phi}}_i = -\gamma_{\phi_i}(\dot{z}_i S_i + \sigma_i \hat{\phi}_i) \tag{23}$$

with γ_{g_i}, η_i, γ_{ϕ_i}, σ_i being positive design parameters. Let x_{i+1d} pass through a first-order filter to obtain z_{i+1}:

$$\tau_{i+1} \dot{z}_{i+1} + z_{i+1} = x_{(i+1)d}, \quad z_{i+1}(0) = x_{(i+1)d}(0) \tag{24}$$

where τ_{i+1} is the time constant.

Step n. Define the n-th surface error

$$S_n = x_n - z_n - c_n \tag{25}$$

with c_n being any design parameter, whose derivative is

$$\dot{S}_n = \dot{x}_n - \dot{z}_n = \beta u + d_n + \theta_n f_n(\bar{x}_n) + \Delta_n - \dot{z}_n \tag{26}$$

where (9) has been used. Let

$$\zeta = \frac{1}{\beta} \tag{27}$$

The control law is designed as

$$u = \hat{\zeta} \bar{u} \tag{28}$$

where $\hat{\zeta}$, which is the estimate of ζ, is updated by

$$\dot{\hat{\zeta}} = -\gamma_\zeta(\bar{u} S_n + \eta_\zeta \hat{\zeta}) \tag{29}$$

with γ_ζ, η_ζ being positive design parameters, and

$$\bar{u} = -k_n S_n - \hat{\theta}_n f_n(\bar{x}_n) - \frac{S_n \rho_n^2(\bar{x}_n)}{2\varepsilon} + \dot{z}_n - \text{sgn}(S_n)\hat{d} \tag{30}$$

where $\hat{\theta}_n$ and $\hat{d}$, which are the estimations of θ_n and d, respectively, are updated by

$$\dot{\hat{\theta}}_n = \gamma_{g_n}(f_n(\bar{x}_n)S_n - \eta_n \hat{\theta}_n) \tag{31}$$
$$\dot{\hat{d}} = \gamma_d(|S_n| - \eta_d \hat{d}) \tag{32}$$

Remark 3. In the above design procedure, the commonly adopted dynamic surfaces, i.e., $S_i = x_i - z_i$ ($2 \le i \le n$), are abandoned. Instead, we use $S_i = x_i - z_i - c_i$ as our dynamic surfaces for the purpose of deriving $\mathcal{L}_\infty$ performance of tracking error, which will be given in the next section.

Remark 4. In comparison with the backstepping design[13, 16, 18], the above design procedure shows that the derivation of low-pass filter at each design step makes the control law quite simple. However, the price we have to pay is that only semiglobal stability can be guaranteed and the tracking error does not converge to zero but to a small residual set.

3 Stability and transient performance analysis

In this section, the stability and transient performance analysis for the proposed DSC scheme will be presented, which develops the technique given by [20]. Although the design procedure is simple, the stability analysis is complicated due to the derivation of the low-pass filters. To this end, define

$$\begin{aligned} y_2 &= z_2 - x_{2d} = \\ &z_2 + \hat{\theta}_{g_1} f_1(x_1) + \frac{1}{g_{\min}} \frac{S_1 \rho_1^2(x_1)}{2\varepsilon} + k_1 S_1 - \hat{\phi}_1 \dot{y}_r \\ y_{i+1} &= z_{i+1} - x_{(i+1)d} = \\ &z_{i+1} + \hat{\theta}_{g_i} f_i(\bar{x}_i) + \frac{1}{g_{\min}} \frac{S_i \rho_i^2(\bar{x}_i)}{2\varepsilon} + k_i S_i - \hat{\phi}_i \dot{z}_i, \\ &i = 2, \cdots, n-1 \end{aligned} \tag{33}$$

where x_{2d} and $x_{(i+1)d}$ are given by (16) and (22), respectively. Further, define the estimation errors

$$\tilde{\theta}_{g_i} = \hat{\theta}_{g_i} - \theta_{g_i} \tag{34}$$
$$\tilde{\phi}_i = \hat{\phi}_i - \phi_i, \quad i = 1, \cdots, n-1 \tag{35}$$
$$\tilde{\theta}_n = \hat{\theta}_n - \theta_n \tag{36}$$
$$\tilde{\zeta} = \hat{\zeta} - \zeta \tag{37}$$
$$\tilde{d} = \hat{d} - d \tag{38}$$

[1] As will be shown in Section 3, the design parameters $c_2, c_3, \cdots, c_n$ in Step i and Step n are used to guarantee $\mathcal{L}_\infty$ performance of the tracking error.

Using (33) $\sim$ (35), we can write (14) and (20) as

$$\dot{S}_1 = -g_1k_1S_1 + g_1S_2 + g_1y_2 + g_1c_2 - g_1\tilde{\theta}_{g_1}f_1(x_1) + g_1\tilde{\phi}_1\dot{y}_r + \Delta_1 - \frac{g_1}{g_{\min}}\frac{S_1\rho_1^2(x_1)}{2\varepsilon}$$

$$\dot{S}_i = -g_ik_iS_i + g_iS_{i+1} + g_iy_{i+1} + g_ic_{i+1} - g_i\tilde{\theta}_{g_i}f_i(\bar{x}_i) + g_i\tilde{\phi}_i\dot{z}_i + \Delta_i - \frac{g_i}{g_{\min}}\frac{S_i\rho_i^2(\bar{x}_i)}{2\varepsilon},\quad i = 2,\cdots,n-1 \tag{39}$$

From (28), we can rewrite βu in (26) as

$$\beta u = \beta\hat{\zeta}\bar{u} = \beta(\tilde{\zeta} + \zeta)\bar{u} = \bar{u} + \beta\tilde{\zeta}\bar{u} \tag{40}$$

Taking (30), (36) $\sim$ (38), and (40) into consideration, (26) can be rewritten as

$$\dot{S}_n = -k_nS_n - \tilde{\theta}_nf_n(\bar{x}_n) + \left(\Delta_n - \frac{S_n\rho_n^2(\bar{x}_n)}{2\varepsilon}\right) + d_n - \mathrm{sgn}(S_n)\hat{d} + \beta\tilde{\zeta}\bar{u} \tag{41}$$

Since

$$\dot{z}_i = \frac{x_{id} - z_i}{\tau_i} = -\frac{y_i}{\tau_i},\quad i = 2,\cdots,n \tag{42}$$

from (33), we obtain

$$\dot{y}_2 = -\frac{y_2}{\tau_2} + \dot{\hat{\theta}}_{g_1}f_1(x_1) + \hat{\theta}_{g_1}\frac{\partial f_1(x_1)}{\partial x_1}\dot{x}_1 + k_1\dot{S}_1 + \frac{1}{g_{\min}}\frac{\dot{S}_1\rho_1^2(x_1)}{2\varepsilon} + \frac{S_1}{g_{\min}\varepsilon}\rho_1(x_1)\frac{\partial\rho_1(x_1)}{\partial x_1}\dot{x}_1 - \hat{\phi}_1\ddot{y}_r - \dot{\hat{\phi}}_1\dot{y}_r = -\frac{y_2}{\tau_2} + B_2(S_1, S_2, y_2, \hat{\theta}_{g_1}, \hat{\phi}_1, y_r, \dot{y}_r, \ddot{y}_r)$$

$$\dot{y}_{i+1} = -\frac{y_{i+1}}{\tau_{i+1}} + \dot{\hat{\theta}}_{g_i}f_i(\bar{x}_i) + \hat{\theta}_{g_i}\sum_{j=1}^{i}\frac{\partial f_i(\bar{x}_i)}{\partial x_j}\dot{x}_j + \frac{1}{g_{\min}}\frac{\dot{S}_i\rho_i^2(\bar{x}_i)}{2\varepsilon} + \frac{S_i}{g_{\min}\varepsilon}\rho_i(\bar{x}_i)\sum_{j=1}^{i}\frac{\partial\rho_i(\bar{x}_i)}{\partial x_j}\dot{x}_j + k_i\dot{S}_i + \hat{\phi}_i\frac{\dot{y}_i}{\tau_i} + \dot{\hat{\phi}}_i\frac{y_i}{\tau_i} = -\frac{y_{i+1}}{\tau_{i+1}} + B_{i+1}(S_1,\cdots,S_{i+1}, y_2,\cdots,y_{i+1}, \hat{\theta}_{g_1},\cdots,\hat{\theta}_{gi}, \hat{\phi}_1,\cdots,\hat{\phi}_i, y_r, \dot{y}_r, \ddot{y}_r) \tag{43}$$

where B_{i+1}, $i = 1,\cdots,n-1$ are continuous functions.

We are now ready to establish the main theorem of this paper.

Theorem 1. Consider the closed-loop system (9), (39), (41), and (43). Let the Lyapunov function candidate be defined as

$$V = \frac{1}{2}\sum_{i=1}^{n-1}\left(\frac{1}{g_i}S_i^2 + \frac{1}{\gamma_{g_i}}\tilde{\theta}_{g_i}^2 + \frac{1}{\gamma_{\phi_i}}\tilde{\phi}_i^2 + y_{i+1}^2\right) + \frac{1}{2}\left(\frac{\beta}{\gamma_\zeta}\tilde{\zeta}^2 + \frac{1}{\gamma_{g_n}}\tilde{\theta}_n^2 + \frac{1}{\gamma_d}\tilde{d}^2 + S_n^2\right) \tag{44}$$

Then for any given positive number p, if $V(0) \le p$, there exist design parameters k_i, τ_{i+1}, γ_{g_i}, γ_{ϕ_i}, γ_ζ, γ_{g_n}, γ_d, η_i, η_n, η_ζ, η_d, σ_i, $i = 1,\cdots,n-1$ such that all the signals of the closed-loop system are uniformly bounded and the tracking error converges to a residual set that can be made arbitrarily small by properly choosing the design parameters. Furthermore, by choosing the design parameters and initializing the dynamic surfaces properly, the $\mathcal{L}_\infty$ norm of the tracking error can be guaranteed.

Proof. The time derivative of V yields

$$\dot{V} = \sum_{i=1}^{n-1}\left(\frac{1}{g_i}S_i\dot{S}_i + \frac{1}{\gamma_{g_i}}\tilde{\theta}_{g_i}\dot{\hat{\theta}}_{g_i} + \frac{1}{\gamma_{\phi_i}}\tilde{\phi}_i\dot{\hat{\phi}}_i + y_{i+1}\dot{y}_{i+1}\right) + S_n\dot{S}_n + \frac{\beta}{\gamma_\zeta}\tilde{\zeta}\dot{\hat{\zeta}} + \frac{1}{\gamma_{g_n}}\tilde{\theta}_n\dot{\hat{\theta}}_n + \frac{1}{\gamma_d}\tilde{d}\dot{\hat{d}} \tag{45}$$

Note that for $i = 1,\cdots,n$, the following inequalities hold:

$$S_i\Delta_i \le |S_i|\,\rho_i(\bar{x}_i) \le \frac{S_i^2\rho_i^2(\bar{x}_i)}{2\varepsilon} + \frac{\varepsilon}{2} \tag{46}$$

Using (39) and (46), we obtain that

$$\frac{1}{g_1}S_1\dot{S}_1 \le (-k_1S_1^2 + S_1S_2 + S_1y_2 + S_1c_2) - \tilde{\theta}_{g_1}f_1(x_1)S_1 + \tilde{\phi}_1\dot{y}_rS_1 + \frac{\varepsilon}{2g_{\min}}$$

$$\frac{1}{g_i}S_i\dot{S}_i \le (-k_iS_i^2 + S_iS_{i+1} + S_iy_{i+1} + S_ic_{i+1}) - \tilde{\theta}_{g_i}f_i(\bar{x}_i)S_i + \tilde{\phi}_i\dot{z}_iS_i + \frac{\varepsilon}{2g_{\min}},\quad i = 2,\cdots,n-1 \tag{47}$$

Similarly, using (41) and (46), it follows that

$$S_n\dot{S}_n \le -k_nS_n^2 + \beta\tilde{\zeta}\bar{u}S_n + S_nd_n - |S_n|\,\hat{d} - \tilde{\theta}_nf_n(\bar{x}_n)S_n + \frac{\varepsilon}{2} \tag{48}$$

In view of (43), (47), (48), and substituting the adaptive laws (17), (23), (29), (31), (32) into (45) yields

$$\dot{V} \le \sum_{i=1}^{n-1}\left(-k_iS_i^2 + S_iS_{i+1} + S_iy_{i+1} + S_ic_{i+1}\right) + \sum_{i=1}^{n-1}\left(-\eta_i\tilde{\theta}_{g_i}\hat{\theta}_{g_i} - \sigma_i\tilde{\phi}_i\hat{\phi}_i\right) - k_nS_n^2 - \eta_\zeta\beta\tilde{\zeta}\hat{\zeta} - \eta_d\tilde{d}\hat{d} - \eta_n\tilde{\theta}_n\hat{\theta}_n + \sum_{i=1}^{n-1}\left(-\frac{y_{i+1}^2}{\tau_{i+1}} + |y_{i+1}B_{i+1}|\right) + \frac{(n-1)\varepsilon}{2g_{\min}} + \frac{\varepsilon}{2} \tag{49}$$

where we have used the inequality $S_nd_n \le |S_n|\,d$. By Assumption 3, the set

$$\Pi = \{(y_r, \dot{y}_r, \ddot{y}_r) : y_r^2 + \dot{y}_r^2 + \ddot{y}_r^2 \le B_1\} \tag{50}$$

is compact in $\mathbf{R^3}$ for some $B_1 > 0$. Moreover, the sets

$$\Pi_i = \left\{\sum_{j=1}^{i}\left(\frac{1}{g_j}S_j^2 + \frac{1}{\gamma_{g_j}}\tilde{\theta}_{g_j}^2 + \frac{1}{\gamma_{\phi_j}}\tilde{\phi}_j^2 + y_{j+1}^2\right) \le 2p\right\},\quad i = 1,\cdots,n-1 \tag{51}$$

$$\Pi_n = \left\{\begin{array}{l}\displaystyle\sum_{i=1}^{n-1}\left(\frac{1}{g_i}S_i^2 + \frac{1}{\gamma_{g_i}}\tilde{\theta}_{g_i}^2 + \frac{1}{\gamma_{\phi_i}}\tilde{\phi}_i^2 + y_{i+1}^2\right) + \\ \displaystyle\frac{\beta}{\gamma_\zeta}\tilde{\zeta}^2 + \frac{1}{\gamma_{g_n}}\tilde{\theta}_n^2 + \frac{1}{\gamma_d}\tilde{d}^2 + S_n^2 \le 2p\end{array}\right\} \tag{52}$$

are compact in $\mathbf{R}^{4i}$ and $\mathbf{R}^{4n}$, respectively. Note that $\Pi\times\Pi_i$ and $\Pi\times\Pi_n$ are also compact in $\mathbf{R}^{4i+3}$ and $\mathbf{R}^{4n+3}$, respectively. Therefore, $|B_{i+1}|$ have maximums, i.e., M_{i+1} on $\Pi\times\Pi_i$. Using the inequalities

$$\begin{aligned}S_iS_{i+1} &\le S_i^2+\frac{1}{4}S_{i+1}^2\\ S_iy_{i+1} &\le S_i^2+\frac{1}{4}y_{i+1}^2\\ S_ic_{i+1} &\le S_i^2+\frac{1}{4}c_{i+1}^2\end{aligned}\tag{53}$$

and taking (53) into consideration, we have

$$\begin{aligned}\dot V \le& \sum_{i=1}^{n-1}\left(-k_iS_i^2+3S_i^2+\frac{1}{4}S_{i+1}^2+\frac{1}{4}y_{i+1}^2+\frac{1}{4}c_{i+1}^2\right)+\\ &\sum_{i=1}^{n-1}(-\eta_i\tilde\theta_{g_i}\hat\theta_{g_i}-\sigma_i\tilde\phi_i\hat\phi_i)-k_nS_n^2-\eta_\zeta\beta\tilde\zeta\hat\zeta-\\ &\eta_d\tilde d\hat d-\eta_n\tilde\theta_n\hat\theta_n+\sum_{i=1}^{n-1}\left(-\frac{y_{i+1}^2}{\tau_{i+1}}+|y_{i+1}B_{i+1}|\right)+\\ &\frac{(n-1)\varepsilon}{2g_{\min}}+\frac{\varepsilon}{2}\end{aligned}\tag{54}$$

In the above inequality, we let

$$\begin{aligned}k_1 &= 3+\frac{\alpha_0}{g_{\min}}\\ k_i &= 3\frac{1}{4}+\frac{\alpha_0}{g_{\min}},\ i=2,\cdots,n-1\\ k_n &= \frac{1}{4}+\alpha_0,\\ \eta_i &= \frac{2\alpha_0}{\gamma_{g_i}},\ i=1,\cdots,n\\ \sigma_i &= \frac{2\alpha_0}{\gamma_{\phi_i}},\ i=1,\cdots,n-1\\ \eta_\zeta &= \frac{2\alpha_0}{\gamma_\zeta}\\ \eta_d &= \frac{2\alpha_0}{\gamma_d}\end{aligned}\tag{55}$$

where α_0 is a positive constant. Also note that

$$\begin{aligned}\tilde\zeta\hat\zeta &= \tilde\zeta^2+\tilde\zeta\zeta\\ \tilde d\hat d &= \tilde d^2+\tilde dd\\ \tilde\phi_i\hat\phi_i &= \tilde\phi_i^2+\tilde\phi_i\phi_i,\ i=1,\cdots,n-1\\ \tilde\theta_{g_i}\hat\theta_{g_i} &= \tilde\theta_{g_i}^2+\tilde\theta_{g_i}\theta_{g_i},\ i=1,\cdots,n-1\\ \tilde\theta_n\hat\theta_n &= \tilde\theta_n^2+\tilde\theta_n\theta_n\end{aligned}\tag{56}$$

Hence, the following equalities hold:

$$\begin{aligned}-\eta_\zeta\beta\tilde\zeta\hat\zeta &\le -\frac{\eta_\zeta\beta}{2}(\tilde\zeta^2-\zeta^2)\\ -\eta_d\tilde d\hat d &\le -\frac{\eta_d}{2}(\tilde d^2-d^2)\\ -\sigma_i\tilde\phi_i\hat\phi_i &\le -\frac{\sigma_i}{2}(\tilde\phi_i^2-\phi_i^2),\ i=1,\cdots,n-1\\ -\eta_i\tilde\theta_{g_i}\hat\theta_{g_i} &\le -\frac{\eta_i}{2}(\tilde\theta_{g_i}^2-\theta_{g_i}^2),\ i=1,\cdots,n-1\\ -\eta_n\tilde\theta_n\hat\theta_n &\le -\frac{\eta_n}{2}(\tilde\theta_n^2-\theta_n^2)\end{aligned}\tag{57}$$

From (54) $\sim$ (57), we obtain that

$$\begin{aligned}\dot V \le& -\alpha_0\sum_{i=1}^{n-1}\left(\frac{1}{g_i}S_i^2+\frac{1}{\gamma_{g_i}}\tilde\theta_{g_i}^2+\frac{1}{\gamma_{\phi_i}}\tilde\phi_i^2\right)-\\ &\alpha_0\left(\frac{\beta}{\gamma_\zeta}\tilde\zeta^2+\frac{1}{\gamma_{g_n}}\tilde\theta_n^2+\frac{1}{\gamma_d}\tilde d^2+S_n^2\right)+\\ &\sum_{i=1}^{n-1}\left(\frac{1}{4}y_{i+1}^2-\frac{y_{i+1}^2}{\tau_{i+1}}+|y_{i+1}B_{i+1}|\right)+\\ &\sum_{i=1}^{n-1}\left(\frac{\eta_i}{2}\theta_{g_i}^2+\frac{\sigma_i}{2}\phi_i^2+\frac{1}{4}c_{i+1}^2\right)+\frac{\eta_n}{2}\theta_n^2+\\ &\frac{\eta_\zeta\beta}{2}\zeta^2+\frac{\eta_d}{2}d^2+\frac{(n-1)\varepsilon}{2g_{\min}}+\frac{\varepsilon}{2}\end{aligned}\tag{58}$$

Notice that for any positive number μ, we have

$$|y_{i+1}B_{i+1}|\le\frac{y_{i+1}^2M_{i+1}^2}{2\mu}+\frac{\mu}{2},\ i=1,\cdots,n-1\tag{59}$$

Let

$$\frac{1}{\tau_{i+1}}=\frac{1}{4}+\frac{M_{i+1}^2}{2\mu}+\alpha_0,\ i=1,\cdots,n-1\tag{60}$$

$$\begin{aligned}e_M =& \sum_{i=1}^{n-1}\left(\frac{\eta_i}{2}\theta_{g_i}^2+\frac{\sigma_i}{2}\phi_i^2+\frac{1}{4}c_{i+1}^2\right)+\frac{\eta_n}{2}\theta_n^2+\\ &\frac{\eta_\zeta\beta}{2}\zeta^2+\frac{\eta_d}{2}d^2+\frac{(n-1)\varepsilon}{2g_{\min}}+\frac{\varepsilon}{2}\end{aligned}\tag{61}$$

Using (59) and (60), we have the following inequality:

$$\begin{aligned}\sum_{i=1}^{n-1}\left(\frac{1}{4}y_{i+1}^2+|y_{i+1}B_{i+1}|-\frac{y_{i+1}^2}{\tau_{i+1}}\right)\le&\\ -\alpha_0\sum_{i=1}^{n-1}y_{i+1}^2+\frac{(n-1)\mu}{2}&\end{aligned}\tag{62}$$

where the left hand side of (62) appears in (58). Replacing (62) in (58) and in view of (61), it follows that

$$\dot V\le -2\alpha_0V+e_M+\frac{(n-1)\mu}{2}\tag{63}$$

Let

$$\alpha_0>\frac{e_M+\dfrac{(n-1)\mu}{2}}{2p}\tag{64}$$

then $\dot V\le 0$ on $V=p$. That is, $V\le p$ is an invariant set, i.e., if $V(0)\le p$, then $V(t)\le p$, for all $t\ge 0$. Solving the inequality (63), we obtain

$$V(t)\le\frac{e_M+\dfrac{(n-1)\mu}{2}}{2\alpha_0}+\left(V(0)-\frac{e_M+\dfrac{(n-1)\mu}{2}}{2\alpha_0}\right)\mathrm{e}^{-2\alpha_0t}\tag{65}$$

which implies that

$$\lim_{t\to\infty}V(t)=\frac{e_M+\dfrac{(n-1)\mu}{2}}{2\alpha_0}\tag{66}$$

Thus, all signals of the closed-loop system, i.e., S_i, $\hat\theta_{g_i}$, $\hat\phi_i$, $\hat\theta_n$, $\hat d$, $\hat\zeta$, y_{i+1}, are uniformly bounded. Moreover, from (55), by appropriately choosing the design parameters γ_{g_i}, γ_{ϕ_i}, γ_{g_n}, γ_ζ, γ_d, k_i, k_n, τ_{i+1}, $i = 1, \cdots, n-1$, we can make α_0 larger, which together with (66) implies that the tracking error can be made arbitrarily small.

Finally, to obtain $\mathcal{L}_\infty$ performance of the tracking error, we set the initial conditions of the parameter estimators in (17), (23), (29), (31), and (32) to zero, i.e.,

$$\begin{aligned} &\hat{\theta}_{g_i}(0) = 0 \\ &\hat{\phi}_i(0) = 0, \quad i = 1, \cdots, n-1 \\ &\hat{\theta}_n(0) = 0 \\ &\hat{\zeta}(0) = 0 \\ &\hat{d}(0) = 0 \end{aligned} \tag{67}$$

and set $S_i(0) = 0$, $i = 1, \cdots, n$, which can be done by letting $y_r(0)$ (see Assumption 3) and the design parameters $c_2, \cdots, c_n$ satisfy

$$\begin{aligned} &y_r(0) = x_1(0) \\ &c_i = x_i(0), \quad i = 2, \cdots, n \end{aligned} \tag{68}$$

Now, taking (67) and (68) into consideration, from (13), (16), (18), (19), (22), (24), (25), (33), and (44), it can be shown in a step-by-step fashion that

$$\begin{aligned} &S_i(0) = 0, \quad i = 1, \cdots, n \\ &x_{(i+1)d}(0) = 0 \Rightarrow z_{i+1}(0) = 0 \\ &y_{i+1}(0) = z_{i+1}(0) - x_{(i+1)d}(0) = 0, \quad i = 1, \cdots, n-1 \end{aligned}$$

$$\begin{aligned} V(0) = &\frac{1}{2}\sum_{i=1}^{n-1}\left(\frac{1}{\gamma_{g_i}}\theta_{g_i}^2 + \frac{1}{\gamma_{\phi_i}}\phi_i^2\right) + \\ &\frac{1}{2}\left(\frac{\beta}{\gamma_\zeta}\zeta^2 + \frac{1}{\gamma_{g_n}}\theta_n^2 + \frac{1}{\gamma_d}d^2\right) \end{aligned} \tag{69}$$

From (55) and (61), it follows that

$$V(0) - \frac{e_M + \dfrac{(n-1)\mu}{2}}{2\alpha_0} < 0 \tag{70}$$

which, together with (65), implies that

$$0 \le V(t) \le \frac{e_M + \dfrac{(n-1)\mu}{2}}{2\alpha_0} \tag{71}$$

Therefore,

$$\|S_1\|_\infty \le \sqrt{g_{\max} \times \frac{e_{M+}\dfrac{(n-1)}{2}\mu}{\alpha_0}} \tag{72}$$

Note that we can first fix η_i, σ_i, $i = 1, \cdots, n-1$, η_n, η_ζ, η_d, μ, then choose the design parameters γ_{g_i}, γ_{ϕ_i}, γ_ζ, γ_d, γ_{g_n}, such that (55) is satisfied. As a result, $[e_M + (n-1)\mu/2]$ is independent of α_0; hence, from (72), it is clear that the $\mathcal{L}_\infty$ norm of the tracking error S_1 can be improved if a larger α_0 is chosen. □

Remark 5. In Theorem 1, we assume that all initial conditions satisfy (51) and (53). However, since p can be arbitrarily large, the condition is not really restrictive.

4 Simulation results

In this section, to illustrate the effectiveness of the proposed scheme, we consider the following second-order controlled plant with unknown backlash-like hysteresis:

$$\begin{aligned} &\dot{x}_1 = g_1 x_2 + \theta_1 f_1(x_1) + \Delta_1(x, t) \\ &\dot{x}_2 = g_2 w(t) + \theta_2 f_2(\bar{x}_2) + \Delta_2(x, t) \\ &y = x_1 \end{aligned} \tag{73}$$

where w is the output of the hysteresis, g_1, g_2 are unknown parameters, and Δ_1, Δ_2 are disturbances. In the simulation, we choose $g_1 = 1$, $g_2 = 1$, $g_{\min} = 1$, $\theta_1 = 0.1$, $\theta_2 = 0$, $f_1(x_1) = x_1^2$, $f_2(\bar{x}_2) = 0$, $\Delta_1 = 0.2\sin(x_2)$, and $\Delta_2 = 0.1(x_1^2 + x_2^2)\sin^3(t)$. Therefore, $\Delta_1 \le \rho_1(x_1) = 0.2$ and $\Delta_2 \le \rho_2(\bar{x}_2) = 0.1(x_1^2 + x_2^2)$. The hysteresis is described by (5) and (6) with actual parameters $\lambda = 1.432$, $\psi = 0.105$, and $\alpha = 1$. The control objective is to make the state $x_1(= y)$ follow the desired trajectory $y_r = \sin(t)$. According to Section 2, the design procedure is as follows.

Step 1. The first surface error is

$$S_1 = x_1 - y_r \tag{74}$$

From (16),

$$x_{2d} = -\hat{\theta}_{g_1} f_1(x_1) - \frac{1}{g_{\min}}\frac{S_1\rho_1^2(x_1)}{2\varepsilon} - k_1 S_1 + \hat{\phi}_1\dot{y}_r \tag{75}$$

where x_{2d} is obtained by (18) and $\hat{\theta}_{g_1}$, $\hat{\phi}_1$ are updated according to (17).

Step 2. The second surface error is

$$S_2 = x_2 - z_2 - c_2 \tag{76}$$

Since (73) is a second-order system, from (28), the control law is

$$u = \hat{\zeta}\bar{u} \tag{77}$$

where $\hat{\zeta}$ is updated by (29),

$$\begin{aligned} \bar{u} = &-k_2 S_2 - \hat{\theta}_2 f_2(\bar{x}_2) - \frac{S_2\rho_2^2(\bar{x}_2)}{2\varepsilon} + \\ &\frac{x_{2d} - z_2}{\tau_2} - \operatorname{sgn}(S_2)\hat{d} \end{aligned} \tag{78}$$

with $\hat{\theta}_2$, $\hat{d}$ being updated by (31) and (32), respectively.

In this simulation, the initial parameters for update laws are $\hat{\theta}_{g_1}(0) = 0.05$, $\hat{\phi}_1(0) = 1$, $\hat{\zeta}(0) = 0.5$, and $\hat{d}(0) = 1$, respectively. In addition, we choose the design parameters $k_1 = 10$, $k_1 = 0.45$, $\gamma_{g_1} = \gamma_{\phi_1} = \gamma_\zeta = \gamma_d = 8$, the small gains $\eta_1 = \eta_\zeta = \eta_d = \varepsilon = \sigma_1 = 0.01$, and the time constant of the low-pass filter $\tau_2 = 0.01$. The initial states are chosen as $x_1(0) = 0.08$ and $x_2(0) = 0.1$, respectively. Therefore, $c_2 = 0.1$. Also, in the simulation, to avoid chattering, the function $\operatorname{sgn}(S_2)$ is replaced by saturation function $\operatorname{sat}(S_2/0.01)$.

To illustrate the effectiveness of the proposed control scheme, the simulation is done under two different circumstances: with and without considering the effect of hysteresis, which is shown in Fig. 2. Fig. 2 clearly shows that the tracking performance becomes poor once the hysteresis compensation is ignored. Figs. 3 and 4 show the control signal and hysteresis output.

Remark 6. It is interesting to compare the control law (78) obtained by using DSC with the backstepping control law given below:

$$\begin{aligned}\bar{u} = & -k_2 z_2 - \hat{\theta}_2 f_2(\bar{x}_2) - \frac{z_2\rho_2^2(\bar{x}_2)}{2\varepsilon} - \text{sgn}(z_2)\hat{d} - \\ & \gamma_{g_1}(f_1(x_1) - \eta_1\hat{\theta}_{g_1})f_1(x_1) - \gamma_{\phi_1}(\dot{y}_r S_1 - \sigma_1\hat{\phi}_1)\dot{y}_r + \\ & \hat{\phi}_1\ddot{y}_r - \hat{g}_1 k_1 x_2 - \hat{g}_1\hat{\theta}_{g_1}\frac{\partial f_1(x_1)}{\partial x_1}x_2 - \hat{g}_1\frac{\rho_1^2(x_1)}{2g_{\min}\varepsilon}x_2 - \\ & \hat{g}_1\frac{z_1\rho_1(x_1)}{g_{\min}\varepsilon}\frac{\partial\rho_1(x_1)}{\partial x_1}x_2 - k_1\hat{\theta}_1 f_1(x_1) - \\ & \hat{\theta}_1\hat{\theta}_{g_1}\frac{\partial f_1(x_1)}{\partial x_1}f_1(x_1) - \hat{\theta}_1\frac{\rho_1^2(x_1)}{2g_{\min}\varepsilon}f_1(x_1) - \\ & \hat{\theta}_1\frac{z_1\rho_1(x_1)}{g_{\min}\varepsilon}\frac{\partial\rho_1(x_1)}{\partial x_1}f_1(x_1) \end{aligned} \tag{79}$$

which shows that even for the second-order system, $\bar{u}$ is much complicated than that of our proposed scheme. The performance using the backstepping control is shown in Figs. 5 and 6 with the same plant parameters and initial conditions as those of the DSC control scheme, from which it is clear that the DSC and backstepping control have similar tracking performance, but the control amplitude by using the DSC is smaller in this example.

5 Conclusion

In this paper, a robust adaptive DSC for the class of uncertain perturbed strict-feedback nonlinear systems preceded by unknown backlash-like hysteresis has been proposed. We have shown that by using the new scheme, the explosion of complexity problem in backstepping design can be eliminated, the semiglobal uniform ultimate boundedness of all closed-loop signals can be guaranteed, and the convergence of the tracking error to an arbitrarily small residual set can be achieved. Moreover, we have shown that by choosing the design parameters and initializing the dynamic surfaces properly, the $\mathcal{L}_\infty$ performance of system tracking error can be guaranteed.

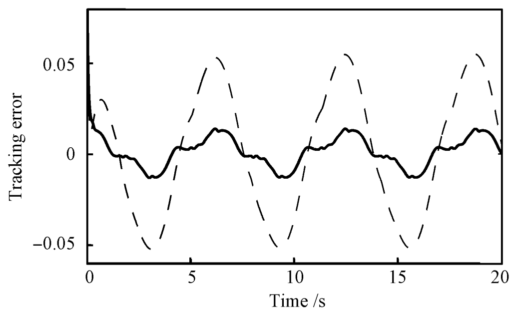

Fig. 2 Tracking errors with (solid line) and without (dashed line) considering hysteresis compensation by using the DSC scheme

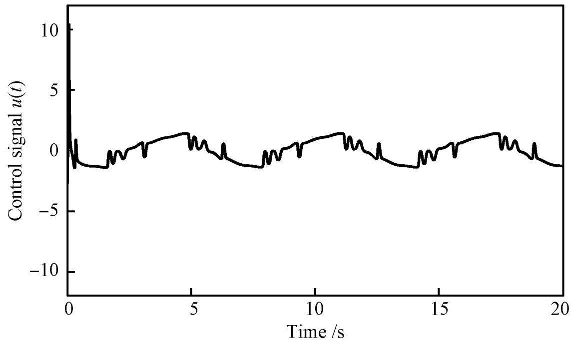

Fig. 3 Control signal $u(t)$ by using the DSC scheme

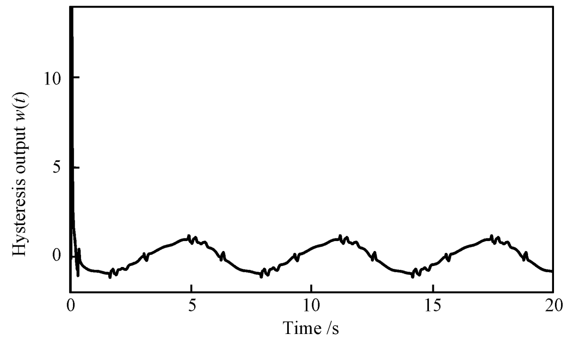

Fig. 4 Hysteresis output $w(t)$ by using the DSC scheme

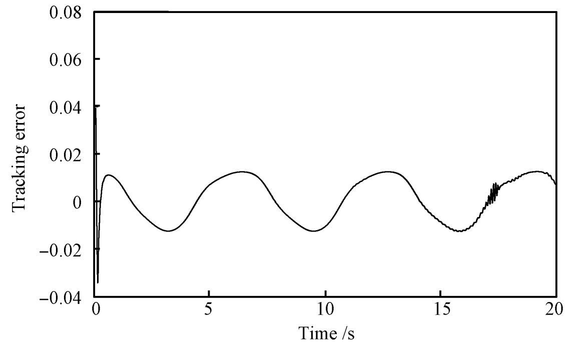

Fig. 5 Tracking error by using backstepping scheme

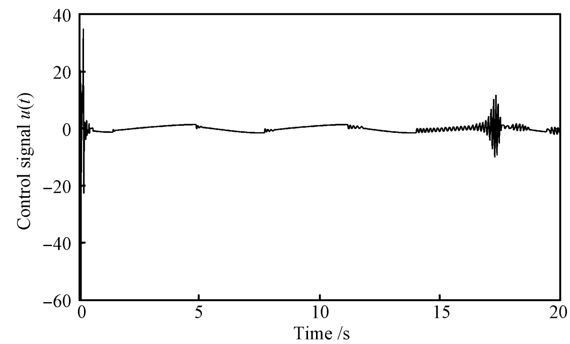

Fig. 6 Control signal $u(t)$ by using backstepping scheme

References

1 Mittal S, Menq C H. Hysteresis compensation in electromagnetic actuators through Perisach model inversion. *IEEE Transactions on Mechatronics*, 2000, **5**(4): 394−409

2 Tan X B, Baras J S. Modeling and control of hysteresis in magnetostrictive actuators. *Automatica*, 2004, **40**(9): 1469−1480

3 Webb G V, Lagoudas D C, Kurdila A J. Hysteresis modeling of SMA actuators for control applications. *Journal of Intelligent Material Systems and Structures*, 1998, **9**(6): 432−448

4 Stepanenko Y, Su C Y. Intelligent control of piezoelectric actuator. In: Proceedings of the 37th Conference on Decision and Control. Tampa, USA: IEEE, 1998. 4234−4239

5 Tao G, Kokotovic P V. Adaptive control of plants with unknown hystereses. *IEEE Transactions on Automatic Control*, 1995, **40**(2): 200−212

6 Moheimani S O R, Goodwin G C. Guest editorial introduction to the special issue on dynamics and control of smart structures. *IEEE Transactions on Control Systems Technology*, 2001, **9**(1): 3−4

7 Tao G, Lewis F L. *Adaptive Control of Nonsmooth Dynamic System*. New York: Springer-Verlag, 2001. 69−83

8 Tan X B, Baras J S. Adaptive identification and control of hysteresis in smart materials. *IEEE Transactions on Automatic Control*, 2005, **50**(6): 827−839

9 Zhang X L, Tan Y H, Su M Y. Modeling of hysteresis in piezoelectric actuators using neural networks. *Mechanical Systems and Signal Processing*, 2009, **23**(8): 2699−2711

10 Wang Q Q, Su C Y. Robust adaptive control of a class of nonlinear systems including actuator hysteresis with Prandtl-Ishlinskii presentations. *Automatica*, 2006, **42**(5): 859−867

11 Xie W F, Fu J, Yao H, Su C Y. Neural network-based adaptive control of piezoelectric actuators with unknown hysteresis. *International Journal of Adaptive Control and Signal Processing*, 2009, **23**(1): 30−54

12 Ahmad N J, Khorrami F. Adaptive control of systems with backlash hysteresis at the input. In: Proceedings of the American Control Conference. San Diego, USA: IEEE, 1999. 3018−3022

13 Su C Y, Wang Q Q, Chen X K, Rakheja S. Adaptive variable structure control of a class of nonlinear systems with unknown Prandtl-Ishlinskii hysteresis. *IEEE Transactions on Automatic Control*, 2005, **50**(12): 2069−2074

14 Su C Y, Stepanenko Y, Svoboda J, Leung T P. Robust adaptive control of a class of nonlinear systems with unknown backlash-like hysteresis. *IEEE Transactions on Automatic Control*, 2000, **45**(12): 2427−2432

15 Chen X K, Hisayama T, Su C Y. Pseudo-inverse-based adaptive control for uncertain discrete time systems preceded by hysteresis. *Automatica*, 2009, **45**(2): 469−476

16 Zhou J, Wen C Y, Zhang Y. Adaptive back-stepping control of a class of uncertain nonlinear systems with unknown backlash-like hysteresis. *IEEE Transactions on Automatic Control*, 2004, **49**(10): 1751−1757

17 Chen X K, Su C Y, Fukuda T. Adaptive control for the systems preceded by hysteresis. *IEEE Transactions on Automatic Control*, 2008, **53**(4): 1019−1025

18 Ren B B, Ge S S, Su C Y, Lee T H. Adaptive neural control for a class of uncertain nonlinear systems in pure-feedback form with hysteresis input. *IEEE Transactions on Systems, Man, and Cybernetics, Part B: Cybernetics*, 2009, **39**(2): 431−443

19 Kanellakopoulos I, Kokotovic P V, Morse A S. Systematic design of adaptive controllers for feedback linearizable systems. *IEEE Transactions on Automatic Control*, 1991, **36**(11): 1241−1253

20 Swaroop D, Hedrick J K, Yip P P, Gerdes J C. Dynamic surface control for a class of nonlinear systems. *IEEE Transactions on Automatic Control*, 2000, **45**(10): 1893−1899

21 Zhang T P, Ge S S. Adaptive dynamic surface control of nonlinear systems with unknown dead zone in pure feedback form. *Automatica*, 2008, **44**(7): 1895−1903

22 Jin Y S, Bae P J, Ho C Y. Adaptive neural control for a class of strict-feedback nonlinear systems with state time delays. *IEEE Transactions on Neural Networks*, 2008, **20**(7): 1209−1215

23 Jin Y S, Bae P J. Neural-network-based decentralized adaptive control for a class of large-scale nonlinear systems with unknown time-varing delays. *IEEE Transactions on Systems, Man, and Cybernetics, Part B: Cybernetics*, 2009, **39**(5): 1316−1323

24 Wang D, Peng Z H, Li T S, Li X Q, Sun G. Adaptive dynamic surface control for a class of uncertain nonlinear systems in pure-feedback form. In: Proceedings of the IEEE Conference on Decision and Control. Shanghai, China: IEEE, 2009. 1956−1961

25 Wei D Q, Luo X S, Wang B H, Fang J Q. Robust adaptive dynamic surface control of chaos in permanent magnet. *Physics Letters A*, 2007, **363**(1-2): 71−77

26 Jin Y S, Bae P J, Ho C Y. Output feedback dynamic surface control of flexible-joint robots. *International Journal of Control Automation and Systems*, 2008, **6**(2): 223−233

27 Chiu P C, Leung T P. Modeling and microcomputer control of a nonlinear pneumatic servomechanism. *Transactions of the Institute of Measurement and Control*, 1998, **10**(2): 71−78

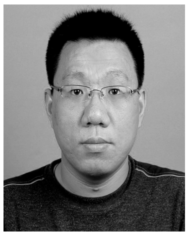

ZHANG Xiu-Yu Received his bachelor and master degrees from North China Electric Power University in 2003 and 2006, respectively. He is currently a Ph. D. candidate at the School of Automation, Beijing University of Aeronautics and Astronautics. His research interest covers robust control and adaptive control.
E-mail: zhangxiuyu80@163.com

LIN Yan Professor at the School of Automation, Beijing University of Aeronautics and Astronautics. His research interest covers robust control and adaptive control. Corresponding author of this paper.
E-mail: linyanee2@yahoo.com.cn